Computing turbulence structure tensors in plane channel flow.

Magnus Vartdal*

Norwegian Defence Research Establishment (FFI), PO Box 25, NO-2027 Kjeller, Norway

Abstract

This paper is concerned with the computation of turbulence structure tensors in plane channel flow. It has been pointed out that the previously computed turbulence structure tensors, for this configuration, used an inconsistent set of boundary conditions. But it was claimed that this had no influence on the computed structure tensors since the velocity field reconstructed by the vector potential only had a constant offset when compared to the original velocity field. In this paper it is shown that this is not the case. Based on a highly resolved LES simulation, the turbulence structure tensors are computed both using the previously employed boundary conditions and a consistent set of boundary conditions. The results exhibit considerable differences in a significant part of the domain.

Keywords:

turbulence structure tensors, vector potential, stream function, plane channel flow

1. Introduction

Turbulent fluid motion consists of many interacting coherent structures commonly referred to as 'eddies'. These eddies vary greatly in size, shape, and kinematic character, the distribution of which is highly case dependent. The type of eddies present in a flow significantly affects its dynamic response to external forcing. In particular, the large energy containing eddies play an active role in the flow dynamics. One way to quantify the turbulence structure of a flow is through two-point correlations of the velocity field. The computation of such correlations can however be exceedingly costly, and one-point

*Email: magnus.vartdal@ffi.no

Dette er en postprint-versjon / This is a postprint version.
DOI til publisert versjon / DOI to published version: 10.1016/j.compfluid.2016.06.007

measures of turbulence structure is therefore desirable from both a flow diagnostic and turbulence modeling perspective.

A comprehensive mathematical framework for structure-describing one-point measures was developed by Kassinos and Reynolds [1]. They introduced the concept of one-point turbulence structure tensors, which have been used for both modeling and turbulence diagnostic purposes [2, 3]. They also demonstrated that two turbulent fields can have the same Reynolds stress and still have different turbulence structure leading to a difference in the interaction between the turbulence and the mean flow field. This means that a description of turbulence based solely on Reynolds stress is fundamentally incomplete. Some turbulence structure information must be included for a complete one-point description.

The definition of turbulence structure tensors is based on the vector potential of the fluctuating velocity field. A prerequisite for computing the tensors is thus the ability to compute the vector potential. While the three-dimensional vector potential has been used in several algorithms involving fluid flow [4, 5, 6, 7, 8, 9, 10], and descriptions of how to compute them for general domains exist [11, 12, 13, 14], the computation of the turbulence structure tensors has, until recently, been limited to simple geometries [2]. Recently, however, a general framework for the computation of the turbulence structure tensors has been proposed [15].

In [15] it was also pointed out that the computations of the structure tensors for turbulent channel flow presented in [2] used an inconsistent set of boundary conditions for the computation of the vector potential. It was claimed that this had no influence on the computed turbulence structure tensors since the velocity field reconstructed by the vector potential only had a constant offset when compared to the original velocity field. In this paper it is shown that this is unfortunately not the case. Based on a highly resolved LES simulation, the turbulence structure tensors are computed both using the previously employed boundary conditions and a consistent set of boundary conditions. The results exhibit considerable differences in a significant portion of the domain.

Dette er en postprint-versjon / This is a postprint version.
DOI til publisert versjon / DOI to published version: 10.1016/j.compfluid.2016.06.007

2. Turbulence structure tensors

Using index notation, the vector potential, ψ_i, commonly called the stream function, is defined by the following relations

$$u_i = \epsilon_{ijk}\psi_{k,j}, \quad \psi_{i,i} = 0, \quad \psi_{i,kk} = -\omega_i, \tag{1}$$

where u_i and ω_i are the fluctuating parts of the turbulent velocity and vorticity fields, respectively, ϵ_{ijk} is the cyclic permutation symbol, and indices found after a comma denote differentiation.

In the above notation, the components of the Reynolds stress, R_{ij}, which are also referred to as the components of componentality, can be expressed in terms of the stream function as follows

$$R_{ij} = \langle u_i u_j \rangle = \epsilon_{ipq}\epsilon_{jrs}\langle \psi_{q,p}\psi_{s,r} \rangle, \tag{2}$$

where $\langle \cdot \rangle$ denotes averaging. By employing the well known relation between the product of cyclic permutation symbols and the Kronecker delta, δ_{ij}, the following constitutive relation is obtained

$$R_{ij} + D_{ij} + F_{ij} - (C_{ij} + C_{ji}) = 2k\delta_{ij}, \tag{3}$$

where $2k = R_{kk}$ is twice the turbulence kinetic energy, and the various structure tensors, and their associated normalized and anisotropic forms, are defined as follows:

Componentality	$R_{ij} = \epsilon_{ipq}\epsilon_{jrs}\langle \psi_{q,p}\psi_{s,r} \rangle$	$r_{ij} = R_{ij}/R_{kk}$	$\tilde{r}_{ij} = r_{ij} - \delta_{ij}/3,$	(4)
Dimensionality	$D_{ij} = \langle \psi_{k,i}\psi_{k,j} \rangle$	$d_{ij} = D_{ij}/D_{kk}$	$\tilde{d}_{ij} = d_{ij} - \delta_{ij}/3,$	(5)
Circulicity	$F_{ij} = \langle \psi_{i,k}\psi_{j,k} \rangle$	$f_{ij} = F_{ij}/F_{kk}$	$\tilde{f}_{ij} = f_{ij} - \delta_{ij}/3,$	(6)
Inhomogenity	$C_{ij} = \langle \psi_{i,k}\psi_{k,j} \rangle$	$c_{ij} = C_{ij}/D_{kk}$	$\tilde{c}_{ij} = c_{ij} - c_{kk}\delta_{ij}/3.$	(7)

The lower case letters represent the normalized tensors and $\tilde{(.)}$ denotes the anisotropic form. The various structure tensors carry complementary statistical information about the turbulence, and detailed discussions of their physical interpretation can be found in [1, 2, 16]. Here, only a short description is provided.

The componentality, or Reynolds stress, provides information about the amplitude of the various components of the fluctuating velocity field. The dimensionality is a measure of the spatial extent of the turbulent structures. A small value of dimensionality means

Dette er en postprint-versjon / This is a postprint version.
DOI til publisert versjon / DOI to published version: 10.1016/j.compfluid.2016.06.007

that there is a large coherence length present in the turbulent field in that direction. This indicates the presence of elongated structures in that direction. The circulicity is a measure of the average large scale circulation in the turbulent field. A large value of circulicity is thus an indicator of the presence of "vortical" eddies with axis oriented in a particular direction. Finally, the inhomogeneity tensor is a measure of the deviation from a homogeneous turbulence state. This interpretation of the inhomogeneity tensor is supported by the observation that equation 7 can be recast, using the Euclid gauge condition ($\psi_{i,i} = 0$), into the following form

$$C_{ij} = \langle \psi_i \psi_{k,j} \rangle_{,k}, \tag{8}$$

which clearly is zero for homogeneous turbulence.

2.1. Anisotropy measures

The anisotropy tensors associated with componentality, dimensionality, and circulicity are symmetric second rank trace-free tensors. This means that they have two independent anisotropy invariants that can be used to characterize the anisotropy state of the tensors. One commonly used set of invariants is

$$II_x = -\frac{1}{2} x_{ij} x_{ji} \tag{9}$$

$$III_x = \frac{1}{3} x_{ij} x_{jk} x_{ki}. \tag{10}$$

For these tensors all possible states fall within the Lumley triangle [17] in $(III_x, -II_x)$-space. One useful way to characterize a turbulent flow is to plot the invariant coordinates for different positions in the physical domain. This results in a graphical representation of the change in turbulence structure as a parametric function of position, which is very useful for analyzing the flow. This method will be employed to highlight the differences in the turbulence structure predicted using the different boundary conditions.

3. Boundary conditions for the vector potential

For general multiply connected domains, such as a plane channel flow, an appropriate set of boundary conditions for the vector potential takes the following form [12, 15]

$$\epsilon_{ijk} \psi_{k,j} = \epsilon_{ijk} n_j u_k \text{ and } n_i \psi_i = 0 \text{ on } \Gamma, \tag{11}$$

Dette er en postprint-versjon / This is a postprint version.
DOI til publisert versjon / DOI to published version: 10.1016/j.compfluid.2016.06.007

where Γ denotes the boundary of the computational domain and n_i is its unit normal.

As pointed out in [15], the computations of the structure tensors for turbulent channel flow presented in [2] used an inconsistent set of boundary conditions for the computation of the vector potential. The boundary conditions used for these calculation were on the form

$$\epsilon_{ijk} n_j \psi_k = 0 \text{ and } \psi_{i,i} = 0 \text{ on } \Gamma. \tag{12}$$

It was then claimed that this had an insignificant effect on the computed turbulence structure tensors, since it only leads to a constant offset of the velocity field reconstructed from the vector potential. This is, however, not the case. A constant velocity field is reconstructed from a stream function with non-zero gradients, which necessarily also changes the turbulence structure tensors.

Consider a turbulent channel flow domain aligned with the coordinate axis such that x is the streamwise coordinate, y is the wall normal coordinate, and z is the spanwise coordinate. A constant velocity field in the streamwise direction is then given by

$$c_i = \epsilon_{ijk} \psi_{k,j}, \tag{13}$$

where $c_i = c\delta_{1i}$ and c is a constant. The vector potential of c_i takes the form

$$\psi_i = cy\delta_{3i} + constant. \tag{14}$$

This yields the following partial derivatives of the vector potential

$$\psi_{i,j} = c\delta_{3i}\delta_{2j}, \tag{15}$$

which is clearly non-zero and will thus contribute to the turbulence structure tensors.

4. Computational setup

A highly resolved LES simulation of a turbulent channel flow with $Re_\tau = 395$ has been carried out on a domain with dimensions $(2\pi H, 2H, \pi H)$, where H is the channel half height. The code used for this simulation was the incompressible flow solver Cliff from Cascade Technologies. It is an unstructured collocated nodal-based finite volume code that solves the primitive variable Navier-Stokes equations using a fractional-step method. It is algorithmically similar to the the CDP code, which is described in [18,

Dette er en postprint-versjon / This is a postprint version.
DOI til publisert versjon / DOI to published version: 10.1016/j.compfluid.2016.06.007

19, 20]. After each step, the required Poisson equations are solved in order to compute the stream function, and the structure tensors are computed based on this calculation. The coordinate system is aligned such that x is the streamwise direction, y is the wall normal direction and z is the spanwise direction. This is the same case as presented in [2]. The number of computational points used in the different directions are $(N_x, N_y, N_z) = (87, 169, 156)$, which results in the near wall resolution $(dx^+, dy^+, dz^+) = (30, 0.4, 8)$.

For this configuration, the structure tensors were computed using both the inconsistent boundary conditions from equation 12 and the consistent boundary conditions found in equation 11. When the boundary conditions in equation 12 are employed, the calculation of the three components of the stream function is decoupled, and its computation is thus carried out by solving three scalar equations. On the other hand, when the boundary conditions in equation 11 are used, the equations for the three components are coupled and the solution of a vector equation is required to determine them. This vector equation can either be solved for all components simultaneously, or an iterative procedure can be used, to reduce memory requirements, as described in [15]. In this paper the simultaneous solution strategy was employed.

The numerical method used to solve the vector Poisson equation deviates slightly from that of [15]. Here the following form of the equation, which is obtained by employing a corollary of Stokes theorem, has been discretized for each control volume

$$\int_{A_p} n_j \frac{\partial \psi_i}{\partial x_j} dA_p + \oint_{C_p} \epsilon_{ijk} t_j \psi_k dc_p = \int_{V_p} -\omega_i dV_p + \int_{S_p} \epsilon_{ijk} n_j u_k dS_p. \tag{16}$$

A_p is the internal part of the surface area associated with the control volume of node p, S_p is the external part of the surface area, V_p is the control volume, C_p is the curve bounding the external part of the surface area, and t_j is the tangent vector to this curve. Using the notation from [15], this is discretized according to

$$\sum_{e' \in E'_p} n_j^{e'} \left. \frac{\partial \psi_i}{\partial x_j} \right|_{e'} A_{e'} + \sum_{f' \in F'} \sum_{e \in \partial f'} \epsilon_{ijk} \pm (x_j^{f'} - x_j^e) \frac{1}{2} (\psi_k^e + \psi_k^F) = -\omega_i V_p + \sum_{f' \in F'} \epsilon_{ijk} n_j^{f'} u_k^{f'} A_{f'}, \tag{17}$$

where the sign of the second term depends on the orientation of the edge. For the channel flow configuration this equation set is discretely equivalent to the method presented in [15].

Dette er en postprint-versjon / This is a postprint version.
DOI til publisert versjon / DOI to published version: 10.1016/j.compfluid.2016.06.007

5. Results

The normalized components of the dimensionality tensor results are shown in Figure 1. They clearly show that the two boundary conditions yield similar results for the d_{11} and d_{12} components in the entire domain, and all components behave similarly towards the center of the channel. Close to the wall, however, very different behavior is observed for the d_{22} and d_{33} components. The inconsistent boundary conditions used in [2], henceforth referred to as $BC1$, result in $d_{22} < d_{33}$, indicating that the spatial coherence length is larger in the wall normal direction than the spanwise direction, while the opposite is true for the consistent boundary conditions, which will be referred to as $BC2$. For $BC2$ the difference between the two components is also larger with a maximum ratio approaching $d_{22}/d_{33} \simeq 3$. Furthermore, for $BC1$ both components have two extremal points very close to the wall ($y^+ \simeq 3.4$ and $y^+ \simeq 11.3$), while $BC2$ only has one extremal point ($y^+ \simeq 12.0$).

The same trend is observed for the circulicity data in Figure 2. The results are similar towards the center of the channel and f_{11} and f_{12} are largely unaffected by the boundary conditions. For the spanwise and wall normal components, differences are again noticeable. For $BC1$, the wall normal component of circulicity dominates close to the wall, while the opposite is true for $BC2$. The number of extremal points are the same as for the dimensionality tensor.

Combining the information in the dimensionality and circulicity tensors, the difference in the predicted near wall turbulence structure using the two different boundary conditions is quite apparent. While both predict structures with elongation in the streamwise direction and small circulicity about this axis, the results differ greatly in the spanwise and wall normal directions. $BC1$ predicts nearly circular jets ($R_{11} >> R_{22}, R_{33}$ not shown here) with a dominant circulation around the wall normal axis. On the other hand, $BC2$ predicts a reduced structure size in the wall normal direction creating a more ellipsoidal shape with a dominant circulation around the the spanwise axis.

The results for the normalized inhomogeneity tensor is shown in Figure 3. Here, a discrepancy between the present results for $BC1$ and those presented in [2] is noted. The present results have a region with large negative values for the c_{22} and c_{33} components close to the wall. This was not evident in the data from [2]. The reason for this deviation

Dette er en postprint-versjon / This is a postprint version.
DOI til publisert versjon / DOI to published version: 10.1016/j.compfluid.2016.06.007

is unknown. Comparing the results for $BC1$ and $BC2$, we see that $BC2$ predicts a slightly wider region with significant inhomogeneity than $BC1$. The main difference is again between the wall normal and spanwise components.

Further information about the difference in turbulence structure, predicted by the two boundary condition sets, can be obtained by considering the anisotropy invariant maps of dimensionality and circulicity found in Figure 4 and 5. For circulicity, the two boundary conditions result in the same overall behavior, but the switch to $BC2$ shifts the extremal points further from the wall. Since the f_{12} component has a relatively large value in a large part of the domain, the coordinate axis are significantly removed from the principal axis of the circulicity tensor in this region. The reversal point, for $BC1$ at $y^+ = 28.92$, is the point at which the dominant direction of circulation switches from the spanwise direction to a direction making an approximate 48° angle with the streamwise direction. This dominant circulation direction is quite stable until $y^+ \simeq 350$, which is close to the channel center.

Figure 4 shows that with $BC2$, the anisotropy state of the dimensionality evolves in a manner similar to the anisotropy of componentality, see [2], although it is slightly shifted away from the $2D - 2C$ line, i.e., the line that represents 2 dimensional and 2 componental turbulence. $BC1$ exhibits a rather peculiar reversal at $y^+ = 3.4$ that seems to be a clear indication that the boundary conditions are yielding erroneous near wall behavior.

6. Conclusion

In this paper it has been demonstrated that the inconsistent boundary conditions that was previously used to compute the vector potential in plane channel flow affects the value of the turbulence structure tensors. This was demonstrated by computing the turbulence structure tensors, from a highly resolved LES simulation, using both the previously employed inconsistent form and a consistent form of the boundary conditions. The results show that the predicted turbulence structure is considerably different in a significant part of the domain with particularly large deviations close to the walls.

Dette er en postprint-versjon / This is a postprint version.
DOI til publisert versjon / DOI to published version: 10.1016/j.compfluid.2016.06.007

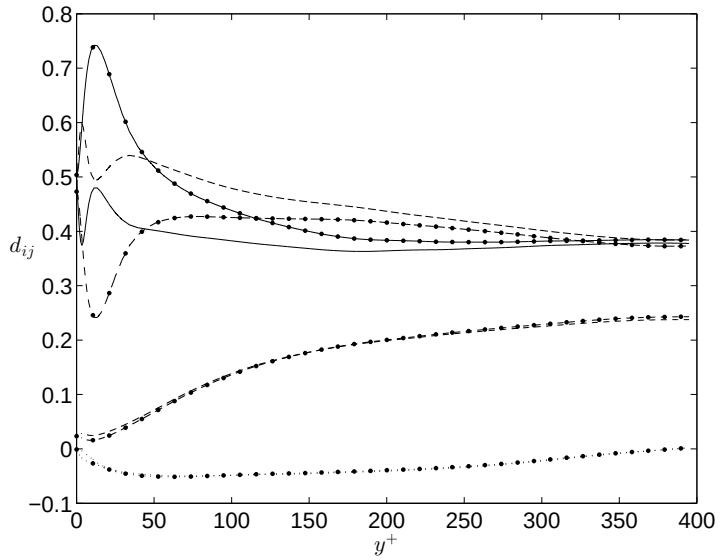

Figure 1: Normalized dimensionality results for half the channel. '– · –', 11 component;'——', 22 component; '- - - -', 33 component; '· · ·', 12 component. Unmarked lines are results using the old formulation of the boundary conditions ($BC1$) and black dots, •, mark results using new boundary conditions ($BC2$).

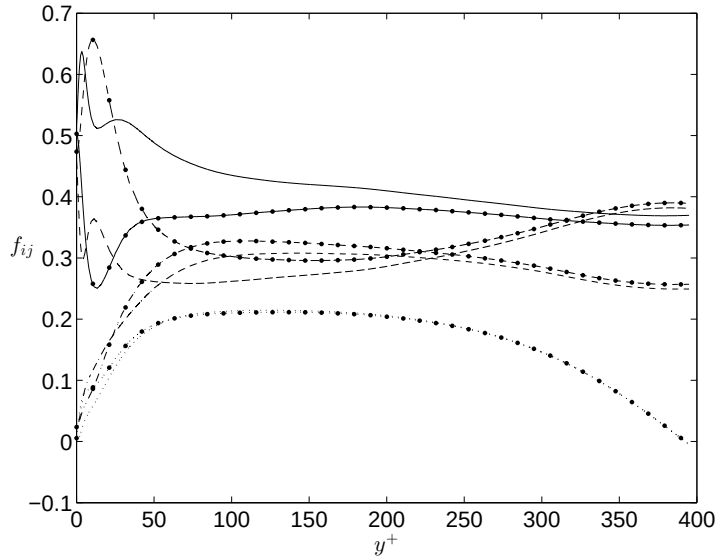

Figure 2: Normalized circulicity results for half the channel. '– · –', 11 component;'——', 22 component; '- - - -', 33 component; '· · ·', 12 component. Unmarked lines are results using the old formulation of the boundary conditions ($BC1$) and black dots, •, mark results using new boundary conditions ($BC2$).

Dette er en postprint-versjon / This is a postprint version.
DOI til publisert versjon / DOI to published version: 10.1016/j.compfluid.2016.06.007

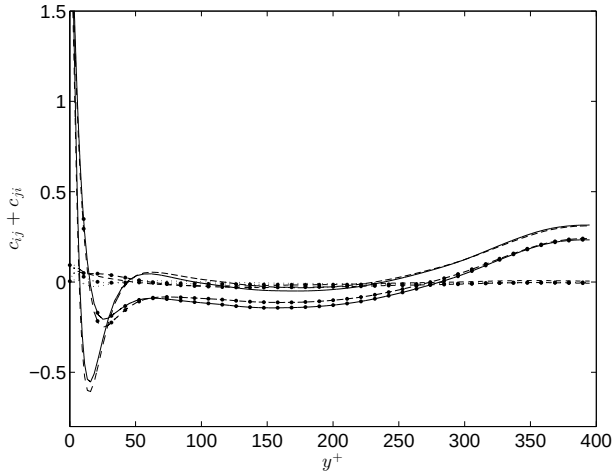

Figure 3: Normalized inhomogeneity results for half the channel. '− · −', 11 component;'——', 22 component; '- - - -', 33 component; '· · ·', 12 component. Unmarked lines are results using the old formulation of the boundary conditions ($BC1$) and black dots, •, mark results using new boundary conditions ($BC2$).

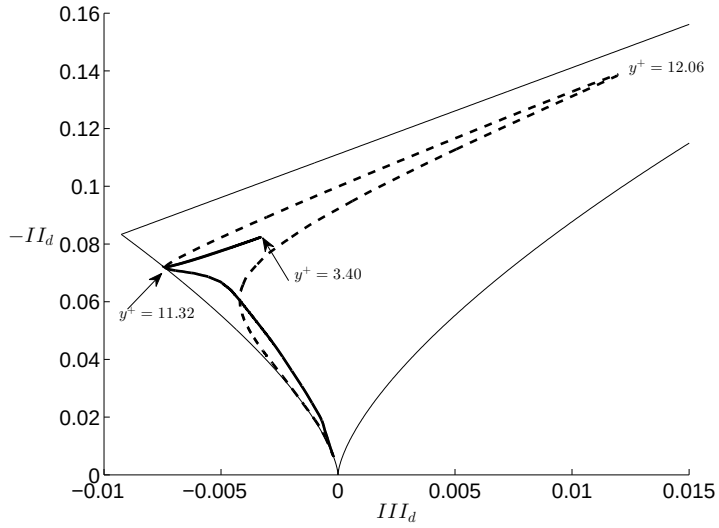

Figure 4: Anisotropy invariant map for dimensionality in half the channel. '——' is the results using the old formulation of the boundary conditions ($BC1$). '- - - -' is the results using the new boundary conditions ($BC2$).

Dette er en postprint-versjon / This is a postprint version.
DOI til publisert versjon / DOI to published version: 10.1016/j.compfluid.2016.06.007

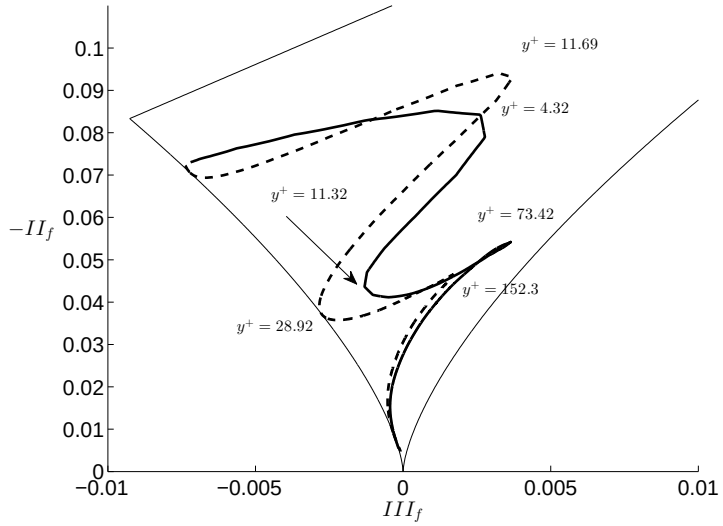

Figure 5: Anisotropy invariant map for circulicity in half the channel. '——' is the results using the old formulation of the boundary conditions ($BC1$). '- - - -' is the results using the new boundary conditions ($BC2$).

7. Acknowledgement

The author would like to thank the reviewer who demonstrated the discrete equivalence, for the channel flow configuration, of the presently used method to that presented in [15]. Furthermore, the author would like to thank Hannibal Fossum for providing the simulation setup of the turbulent channel flow. The author is grateful for the many discussions with Bjørn Anders Pettersson Reif, Carl Erik Wasberg, Thor Gjesdal, Øyvind Andreassen and Emma Wingstedt.

Dette er en postprint-versjon / This is a postprint version.
DOI til publisert versjon / DOI to published version: 10.1016/j.compfluid.2016.06.007

[1] S. C. Kassinos, W. C. Reynolds, A structure-based model for the rapid distortion of homogeneous turbulence, Ph.D. thesis, Department of Mechanical Engineering. Stanford University (1995).

[2] S. C. Kassinos, W. C. Reynolds, M. M. Rogers, One-point turbulence structure tensors, Journal of Fluid Mechanics 428 (2001) 213–248.

[3] D. Grigoriadis, C. Langer, S. Kassinos, Diagnostic properties of structure tensors in turbulent flows, in: Direct and Large-Eddy Simulation VII, Springer, 2010, pp. 41–47.

[4] G. J. Hirasaki, J. Hellums, A general formulation of the boundary conditions on the vector potential in three-dimensional hydrodynamics, J. Soc. Indust. Appl. Math 26 (3).

[5] S. Richardson, A. Cornish, Solution of three-dimensional incompressible flow problems, Journal of fluid Mechanics 82 (02) (1977) 309–319.

[6] A. Wong, J. Reizes, An effective vorticity-vector potential formulation for the numerical solution of three-dimensional duct flow problems, Journal of Computational Physics 55 (1) (1984) 98–114.

[7] O. Tutty, On vector potential-vorticity methods for incompressible flow problems, Journal of Computational Physics 64 (2) (1986) 368–379.

[8] A. Wong, J. Reizes, The vector potential in the numerical solution of three-dimensional fluid dynamics problems in multiply connected regions, Journal of Computational Physics 62 (1) (1986) 124–142.

[9] F. El Dabaghi, O. Pironneau, Stream vectors in three dimensional aerodynamics, Numerische Mathematik 48 (5) (1986) 561–589.

[10] J.-G. Liu, et al., Finite difference methods for 3d viscous incompressible flows in the vorticity–vector potential formulation on nonstaggered grids, Journal of Computational Physics 138 (1) (1997) 57–82.

[11] F. Dubois, Discrete vector potential representation of a divergence-free vector field in three-dimensional domains: Numerical analysis of a model problem, SIAM journal on numerical analysis 27 (5) (1990) 1103–1141.

[12] L. Quartapelle, Numerical solution of the incompressible Navier-Stokes equations, Vol. 113, Springer, 1993.

[13] C. Amrouche, C. Bernardi, M. Dauge, V. Girault, Vector potentials in three-dimensional non-smooth domains, Mathematical Methods in the Applied Sciences 21 (9) (1998) 823–864.

[14] F. Rapetti, F. Dubois, A. Bossavit, Discrete vector potentials for nonsimply connected three-dimensional domains, SIAM journal on numerical analysis 41 (4) (2003) 1505–1527.

[15] F. Stylianou, R. Pecnik, S. Kassinos, A general framework for computing the turbulence structure tensors, Computers & Fluids 106 (0) (2015) 54 – 66.

[16] A. Bhattacharya, S. C. Kassinos, R. D. Moser, Representing anisotropy of two-point second-order turbulence velocity correlations using structure tensors, Physics of Fluids (1994-present) 20 (10) (2008) 101502.

[17] J. L. Lumley, G. R. Newman, The return to isotropy of homogeneous turbulence, Journal of Fluid Mechanics 82 (01) (1977) 161–178.

[18] K. Mahesh, G. Constantinescu, P. Moin, A numerical method for large-eddy simulation in complex

Dette er en postprint-versjon / This is a postprint version.
DOI til publisert versjon / DOI to published version: 10.1016/j.compfluid.2016.06.007

geometries, Journal of Computational Physics 197 (1) (2004) 215 – 240.

[19] F. Ham, G. Iaccarino, Energy conservation in collocated discretization schemes on unstructured meshes, Annual Research Briefs 2004 (2004) 3–14.

[20] F. Ham, K. Mattsson, G. Iaccarino, Accurate and stable finite volume operators for unstructured flow solvers, Annual Research Briefs, Center for Turbulence Research, NASA Ames/Stanford University (2006) 243–261.

Dette er en postprint-versjon / This is a postprint version.
DOI til publisert versjon / DOI to published version: 10.1016/j.compfluid.2016.06.007